BIODIVERSITAS
Volume 26, Number 5, May 2025
Pages: 2383-2392

ISSN: 1412-033X
E-ISSN: 2085-4722
DOI: 10.13057/biodiv/d260535

Identification and genetic diversity of Japanese apricot (*Prunus mume*) accessions in northern Vietnam

THI TUYET CHAM LE[1], THI MAI ANH VU[1], THI THUY HANG VU[1], THI NGOC PHAM[1], DANG DUNG HOANG[2], THU THUY DOAN[1,♥]

[1]Department of Plant Genetics and Breeding, Faculty of Agronomy, Vietnam National University of Agriculture. Trau Quy, Gia Lam 12400, Hanoi, Vietnam. Tel./fax.: +84-4-3666888, ♥email: doanthuy@vnua.edu.vn
[2]Center for Experiment and Vocational Training, Vietnam National University of Agriculture. Trau Quy, Gia Lam 12400, Hanoi, Vietnam

Manuscript received: 4 December 2024. Revision accepted: 11 May 2025.

Abstract. *Le TTC, Vu TMA, Vu TTH, Pham TN, Hoang DD, Doan TT. 2025. Identification and genetic diversity of Japanese apricot* (Prunus mume) *accessions in northern Vietnam. Biodiversitas 26: 2383-2392.* Japanese apricot (*Prunus mume*) is a valuable stone fruit crop grown in northern Vietnam, but lacks comprehensive identification and genetic diversity data. This study aimed to identify species and assess the genetic diversity of Japanese apricot accessions from these regions. A rigorous of agro-morphological traits and *ycf1* sequence analysis was applied to identify *P. mume* plants. The genetic diversity of these 30 collected *P. mume* accessions was analyzed using 19 SSR markers, ensuring a comprehensive understanding of the species. The agro-morphological comparison showed that the Japanese apricot was distinguished from the closely related species (*Prunus salicina*) in several characteristics, including a later flowering time, shorter leaf length, smaller fruit size, and lower flesh rate, but higher Brix. Sequence alignments of the *ycf1* gene revealed that the Japanese apricot differed from close species by nine autapomorphic characters and clustered within the *P. mume* clade. Microsatellite analysis for the 30 *P. mume* accessions exhibited a moderate polymorphism (PIC = 0.41). PCoA and STRUCTURE analysis grouped 30 accessions into NM (18 accessions) and RD (12 accessions) populations according to geographic origin. In summary, the Japanese apricot was recognized as a *P. mume* species, and 19 SSR markers are informative for assessing the Japanese apricot's genetic diversity in Vietnam.

Keywords: Barcode marker, genetic diversity, Japanese apricots, *Prunus mume,* Vietnam

INTRODUCTION

Japanese apricot (*Prunus mume* (Siebold) Siebold & Zucc.), also known as mei fruit, is native to China and is cultivated in Japan, Korea, northern Laos, and northern Vietnam (Moore and Yoneda 2022; POWO 2025). The species is believed to have been domesticated first in China before being transferred to Japan over 2,000 years ago (Numaguchi et al. 2020). Due to their high acidic content, fresh fruits are commonly used in processed products such as wine, pickles, syrups, jam, and ornamental flowers (Yoon et al. 2019; Suwannachot et al. 2021; Li et al. 2022; Moore and Yoneda 2022). Japanese apricot (*Prunus mume*), apricot (*P. armeniaca* L.), plums (*P. domestica* L.), peach (*P. persica* (L.) Stokes), and almond (*P. dulcis* (Mill.) D.A.Webb) are all classified within the subgenus *Prunus* (Moustafa and Cross 2019).

The complex and close phylogenetic relationship between the Japanese apricot (*P. mume*) and the Japanese plum (*P. salicina* Lindl.), attributed to apomixis and natural hybridization, highlights shared interspecific morphologies (Morimoto et al. 2019; Xue et al. 2019). Therefore, reliable and time-efficient methods for identifying Japanese apricot cultivars are essential for species differentiation, conservation, and utilization. Identification of *Prunus* species can be resolved using DNA barcodes like Internal Transcribed Spacer (ITS), *LEAFY*, *rbc*L, *mat*K, *ycf1* (Dong et al. 2015; Hürkan 2020; Sevindik et al. 2024), and/or *trn*L-*trn*F, *trn*H-*psb*A, and *rps*16-*trn*Q, etc.) (Batnini et al. 2019; Halász et al. 2023; Sayed et al. 2023). Among these, gene *ycf1* has demonstrated significant discriminatory power, making it a promising molecular barcode of land plants, such as species in the *Prunus* sect. *Armeniaca* (Rosaceae), *Quercus* (Fagaceae), etc. (Dong et al. 2015). Furthermore, the *ycf1* coding gene was recommended as the most promising DNA barcode for *P. persica* (Amar 2020).

SSR makers have been widely used to study genetic diversity in *Prunus* species, such as peach (*P. persica*), apricot (*P. mume*, *P. armeniaca*), and Japanese plum (*P. salicina*) (Gao et al. 2004; Hayashi et al. 2008; Dettori et al. 2015; Li et al. 2018; Numaguchi et al. 2019; Chen et al. 2022; Guerrero et al. 2022; Kumar et al. 2023). Gao et al. (2004) analyzed 24 Japanese apricot germplasm using 14 SSR markers, indicating no significant genome differences between Chinese and Japanese cultivars (Gao et al. 2004). Hayashi et al. (2008) grouped 127 Japanese apricot accessions into three clusters using 58 SSR markers. Numaguchi et al. (2019) developed 201 SSR markers based on the *P. mume* reference genome, of which 20 SSR markers were highly polymorphic and successfully used to fingerprint 124 *P. mume* accessions.

Japanese apricot is primarily grown in northern provinces of Vietnam with subtropical climates, such as Son La, Lang Son, Lao Cai, Bac Kan, Ha Giang, Quang Ninh (northern mountain region), and Hanoi (Red River delta). Japanese apricot accessions cultivated in Vietnam

are mainly grown for their fruit. Depending on the specific variety, fruit weight typically ranges from 12 to 25 g (Nguyen Huu Hai 2024). According to the classification system indicated by Numaguchi et al. (2023), Japanese apricots are divided into three categories based on fruit weight: small fruits (less than 10 g), medium fruits, and large fruits (over 50 g). Under this system, Vietnamese apricot accessions are classified as medium-sized. These accessions are notably diverse and are commonly distinguished either by their fruit characteristics—such as yellow apricots, peach apricots, rice apricots, and hairy apricots, etc. - or by their growing regions, including Huong Tich apricots from Huong Son, My Duc in Hanoi, and Bac Kan yellow apricots from Bac Kan province etc.

However, no studies have assessed the genetic variation of Japanese apricot (*P. mume*) germplasm in Vietnam. Despite its historical implications, conventional categorization, and diverse uses, studies on the Japanese apricots' genetic background and variation remain limited in Vietnam. Thus, this study aimed to identify Japanese apricot plants and investigate the genetic diversity of Japanese apricot accessions in northern Vietnam.

MATERIALS AND METHODS

Plant materials

The phenotypic observation was conducted on 19 accessions, including 16 *P. mume* accessions/trees in the Red River delta (My Duc District-Hanoi) (Table 1) and three *P. salicina* accessions/trees over two years (2021 and 2022). Five *P. mume* accessions, named 5-RD, 14-RD, 15-RD, 29-RD, and 50-RD, and one *P. salicina* accession (SM5 DongMD) collected from Hanoi (Red River delta region) were used for DNA barcoding. These accessions were selected for analysis due to their differing flowering times. In addition, thirty *P. mume* accessions were collected between 2021 and 2022 from two ecological regions in northern Vietnam: the northern mountain region (14 accessions), including northeast (NE) and northwest (NW), and the Red River delta (16 accessions) (RD) (Table 1, Figure 1) for analysis of genetic diversity.

Table 1. Distribution and number of Japanese apricot accessions collected from two ecological regions in northern Vietnam

Ecological region	Site code	No. of accessions	Serial no/Accessions
Red River delta	RD	16	1 (5-RD), 2 (6-RD), 3 (7-RD), 4 (8-RD), 5 (10-RD), 6 (11-RD), 7 (12-RD), 8 (13-RD), 9 (14-RD), 10 (15-RD), 11 (18-RD), 12 (28-RD), 13 (29-RD), 14 (30-RD), 15 (48-RD), 16 (50-RD)
Northern Mountain (includes northwest (NW) and northeast (NE)	NW, NE	14	17 (52-NE), 18 (56-NE), 19 (60-NE), 20 (62-NE), 21 (66-NW), 22 (67-NW), 23 (70-NW), 24 (71-NW), 25 (73-NW), 26 (74-NW), 27 (75-NW), 28 (76-NE), 29 (77-NE), 30 (79-NE)

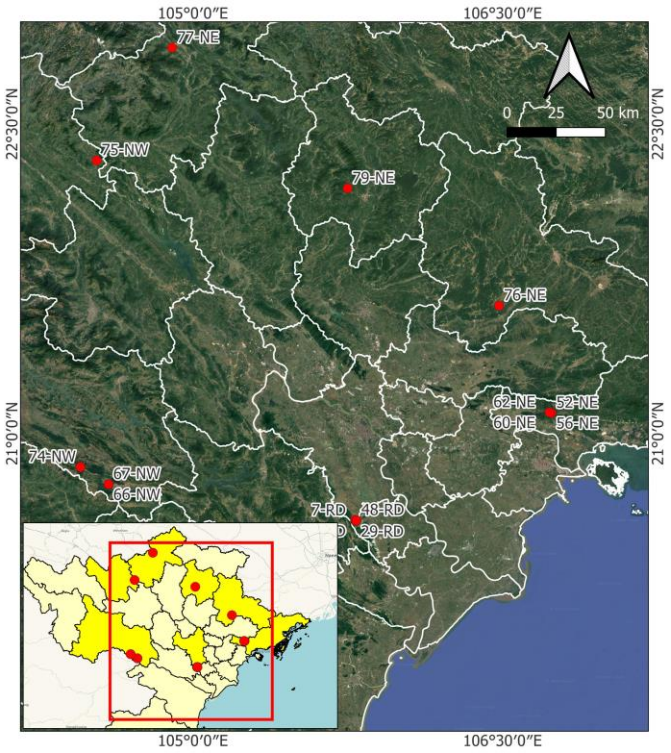

Figure 1. Collection sites of *Prunus mume* accessions in the northern mountain region and in the Red River delta region, northern Vietnam, Vietnam. Each dot presents an accession with a number referring to the collection number and letters denoting the regions (see Table 1)

Phenotypic observation

Fourteen agro-morphological characters were observed and measured at three key stages: flowering (December-January), fruit setting (March-April), and harvest (April) each year. Leaf characteristics included leaf length and width. Fruit characteristics included fresh fruit weight, fruit stone weight, and measurement of fruit and stone dimensions (transversal, longitudinal, and lateral height) (Coulibaly et al. 2022; Numaguchi et al. 2023)

Ten leaves and ten fruits for each plant were collected and brought to the Plant Genetics and Breeding Laboratory, Vietnam National University of Agriculture, Hanoi, for measurement. Fruit samples were harvested at the maturity stage, determined by the fruit's color change from green to yellow. Fully ripened fruits had yellow skin for *P. mume* accessions and orange-yellow skin for *P. salicina* accessions. Total soluble solid contents were measured on fully-ripened fruits using a Brix Meter (Master refractometer, Atago Ajon Company, Tokyo, Japan) (Coulibaly et al. 2022).

Molecular analysis

DNA extraction

Fresh leaves from all accessions were carefully collected, sealed, and transported to the laboratory for subsequent DNA extraction. Total genomic DNA was isolated using a silica membrane according to the instruction manual from the i-genomic Plant DNA Extraction Mini Kit Intron (Korea). The quantity and quality of the DNA were checked using a Nanodrop One spectrophotometer (Thermo Scientific) at 260 nm and 280 nm wavelengths. The extracted DNA was then kept at -20°C for further analysis.

DNA barcoding

Each PCR reaction was conducted in a total reaction volume of 25 µL, containing 0.5 µL each of the primer pair (10 µM) targeting the *ycf1* gene (Forward primer (5'-3' TCTCGACGAAAATCAGATTGTTGTGAAT and reverse primer (5'-3') ATACATGTCAAAGTGATGGAAAA) (Dong et al. 2015), 10 µL DNA polymerase 1U (My Taq HS Mix, Bioline, England) and 0.5 µL DNA template (50ng/µL). The PCR cycling conditions were initiated by predenaturation at 95°C for 3 minutes, followed by 35 cycles of denaturation at 95°C for 30 seconds, annealing at 52°C for 30 seconds, and extension at 72°C for 30 seconds, and finally extended at 72°C for 10 minutes. The amplified fragments for barcode analysis were sent to the National Key Laboratory of Gene Technology (Institute of Biotechnology, Vietnam Academy of Science and Technology, Vietnam) for purification and sequencing.

SSR markers

Thirty *P. mume* accessions were genotyped using 19 SSR markers (Table 2) (Numaguchi et al. 2019). DNA amplification was performed using a thermal cycler (Mastercycler nexus GX2, Eppendorf, Germany) in a volume of 25 µL per each PCR reaction (10 µM each forward and reverse primers (0.5 µL), 10 µL My Taq HS mix 1U (Bioline, England) and 50 ng of template DNA (0.5 µL)). The PCR cycling conditions were initiated by predenaturation at 95°C for 5 minutes, followed by 30 cycles of denaturation at 95°C for 30 seconds, annealing at 55°C for 30 seconds, and extension at 72°C for 30 seconds, and finally extended at 72°C for 10 minutes.

PCR products were separated on a 2% (w/v) agarose gel containing 0.5 mg/mL Redsafe (Intron, Korea) and detected by GelDoc Imaging System (Biorad). Amplicon sizes were determined using a 1 kb DNA ladder (Cleaver, England) as the standard-size marker.

Data analysis

Quantitative traits such as leaf size, fruit weight, stone dimensions, and total soluble solid content were collected in 2021 and 2022. The results primarily focus on the dataset from this year due to the large sample size collected for all 14 traits in 2021. Mean differences between the two groups were conducted using a Student's T-test with a significant level of $p<0.05$ (Student 1908).

Table 2. Primer pairs of 19 SSR markers were used in this study

Marker name	Forward primer (5'-3')	Reverse primer (5'-3')	Linkage group	References
PMKS15	ATGAGGTGGCACATGGTTGA	ACGGTGTGTATTCAGGCTGT	LG1	Numaguchi et al. (2019)
PMKS21	TATGACCACCACCGCAGAAA	AGGGAAGCGAAGATCTGGGA	LG1	
PMKS49	TGACAGGTCATCATACCATTTGGT	GCATGCTGACTCCTCCGAAT	LG2	
PMKS59	GCCCTTTAATCCCAAGGAAGC	AACGAGCCCTAGGGTGTTTG	LG2	
PMKS68	GCAACGTGAGGAAGAGAGGA	CCTTTCATGCAGTGGAGTGG	LG3	
PMKS75	TGGGGAGTTCCTGTCCATGA	AGCACCAGTTAACACCAGCA	LG3	
PMKS99	TCACCCCTCCTCTCTCTTGG	TGCAGAAACATTTGGTGGGA	LG4	
PMKS113	TCTTCTAAGTCAAATGCCTGCCT	TAAGGGATACAGCGGGGTCA	LG4	
PMKS121	AGAAATGCGGAGGTGTAGTGT	GACCTGCAGACAAAATGAGCA	LG5	
PMKS131	GCACCATTCTTTACCACCGC	ACAAGTCAAGTGAAACTCTGCA	LG5	
PMKS133	CCACTCACAGATCGACACGT	GTCAGGTTTGCTGCTGGTTG	LG5	
PMKS149	AGGATCATGGGCAGAAGTTGT	AAGAAGTTGGACTGGGTGCC	LG6	
PMKS164	AAGGGAGGGGACTTCGGTTA	CATCCCAGACGCAATCACCA	LG6	
PMKS175	TGGTTAAGCCACCCATGAGAG	AGCTTTTCCAACCACAACTCA	LG7	
PMKS179	AAATCTCAGGTTGCGTCCCC	ACCCCAAAATGTCATCATCGA	LG7	
PMKS187	TCCCAAACCACCCTTTTCCC	GGGTCTGCAGTCTACACAGG	LG8	
PMKS191	ATTGTGACCCAAGTCCGCAT	TGCACGGGGTGGTGTACTAT	LG8	
PMKS193	TTTCTGTGCCTTGCATTGCC	GCTAGCTGGTCATTGTTGCG	LG8	
PMKS197	CCTCAGGTTCACAAATTGCACA	ACACAGGTATCTGGTCCCGA	LG8	

The sequence data were analyzed and aligned using the MEGA X software package (version 3.6). The *ycf1* gene sequences were used to construct the phylogenetic tree using the Maximum Likelihood (ML) method with a Kimura 2-parameter model and a bootstrap value of 1000. Other *Prunus* accessions with available *ycf1* gene sequences from the NCBI database were included in the analysis. These consisted of four *P. mume* accessions (KP089824.1; MH700953.1; MW755970.1; ON478192.1), one *P. persica* accession (KP88340.1), one *P. armeniaca* accession (KF154906.1), and six *P. salicina* accessions (MW406472.1, NC047442.1; OM256485.1; OR497836.1; OR726647.1, KY420002.1). *Malus halliana* Koehne (Crab apple, KP088297.1) was used as an outgroup for the analysis.

Since SSR markers are codominant, the codominance information for each locus is presented in 2 columns. Alleles are numbered (e.g., 1, 2, 3, ...), as instructed by Peakall and Smouse (2012). The resulting genotype matrix was used as input for statistical analysis of diversity, population structure, and differentiation among the 30 collected *P. mume* accessions. Basic statistics for diversity measurements among the 30 *P. mume* accessions at each SSR locus were calculated using GenAlEx 6.5. These measurements included the total number of alleles (Na), expected heterozygosity (HE), inbreeding coefficient (FIS), and observed heterozygosity (HO).

Polymorphism Information Content (PIC) was calculated by Botstein et al. (1980) as follows:

$$PIC = 1 - \sum_{n=1}^{n} P_i^2$$

Where:

n : Number of alleles

p_i : Frequency of present allele

Based on SSR data, a genetic distance matrix was created for PcoA analysis in GenAlEx 6.5. The pattern of the genetic relationship of Japanese apricot accessions was visualized on a Principal Coordinate Analysis (PCoA) plot.

The population structure of the 30 accessions was determined using STRUCTURE 2.3.4 with the model-based Bayesian (Pritchard et al. 2000). The optimal number of population clusters (K-value) and the estimated membership fraction (Q value) were detected following the ad-hoc ΔK method (Evanno et al. 2005) based on SSR genotypic data. The number of genetic clusters (K) was set from 1 to 10, and each analysis was allowed to run for 100,000 simulations after a burn-in period of 100,000 iterations. Ten runs were performed for each K value. The optimal K value was determined using log probability of data (L(K)), absolute values of the second order rate of change of the likelihood distribution (|L"(K)|), and Delta K (ΔK= mean (|L"(K)|)/sd(L(K)) (Evanno et al. 2005). A representative bar plot for each K value was selected based on LnP(D) values and visualized using Structure Plot v2.0.

RESULTS AND DISCUSSION

Phenotypic characteristics of *P. mume* and *P. salicina*

The comparison of phenotypic characteristics confirmed the distinctiveness of the two species (*P. mume* and *P. salicina*) (Table 3; Figure 2). *P. mume* accessions differed from *P. salicina* accessions in several key traits. *P. salicina* exhibited earlier flowering time (December-January), longer leaf length, larger fruit size, and a higher flesh rate. The total soluble solid content (Brix) in the fruits of *P. salicina* accessions was lower than that in *P. mume* accessions. The leaf length and width differed significantly ($p<0.05$) between *P. mume* accessions (6.42±0.20) and *P. salicina* accessions (7.90±1.36). At the same time, the leaf width of the Japanese apricot group grown in Vietnam is similar to its group in the study of Coulibaly et al. (2022); the leaf length is only equal to the leaf length of the small-fruit group. Besides, the Japanese apricots and plums grown in Vietnam had a small stone weight of 1.21±0.55 g and 1.27±0.06 g, respectively. These stone weights were smaller than the Japanese apricot group grown in China (Coulibaly et al. 2022). However, the stone weight is highly correlated to the apricot fruit weight (Yaegaki et al. 2003). The average Japanese apricot fruit grown in northern Vietnam weighed 11.70±0.78 g. Thus, the percentage of stone/fruit weight ratio is 10% (for Japanese apricot), which is similar to the ratio found in the studies of Yaegaki et al. (2003) and Morimoto et al. (2022) (except for the Elching cultivar originating from Taiwan). However, this percentage was lower than that found in the study of Coulibaly et al. (2022). Due to the low percentage of stone/fruit weight, the fruit flesh rate was high at 89.87%, meeting the requirements for the production of pickled apricots.

The TSS ranged from 9.90±0.42% in *P. salicina* to 11.80±0,67% in *P. mume* (Table 3). This TSS in Japanese apricots here was higher than in most cultivars in the study of Coulibaly et al. (2022), Liu et al. (2022), and Gao et al. (2025). The results showed that the *P. mume* and *P. salicina* accessions differed phenotypically. Figure 2 illustrates the changes in the fruit color from green to full ripening between *P. mume* and *P. salicina* accessions.

Table 3. Comparison of phenotypic characteristics of *P. mume* and *P. salicina* accessions. Measured traits were observed and averaged over two years, 2021 and 2022

Characteristics	*Prunus mume*	*Prunus salicina*
Flowering time	7 Jan-21 Jan	25 Dec-10 Jan
Physiological ripening time	30 Mar-15 Apr	25 Apr-10 May
Leaf length (cm)±SE	6.42±0.20	7.90*±1.36
Leaf width (cm)±SE	3.38±0.42	3.54*±0.99
Fruit weight (g)±SE	11.70±0.78	15.18*±2.69
Fruit stone weight (g)±SE	1.21±0.55	1.27±0.06
Flesh rate (%)±SE	89.87±0.80	91.6*±1.10
Longitudinal height (cm)±SE	3.14±0.56	3.38*±0.26
Transversal height (cm)±SE	3.06±0.56	3.25*±0.31
Lateral height (cm)±SE	2.98±0.50	3.29*±0.20
Stone height (cm)±SE	1.48±0.13	1.91*±0.04
Stone width (cm)±SE	1.40±0.12	1.59*±0.06
Fruit color (at fully ripened stage)	Yellow	Orange-yellow
Total soluble solid content (%)±SE	11.80*±0.67	9.90±0.42

Note: *: Indicating a significant difference between *P. mume* and *P. salicina* accessions at $p<0.05$ (n = 19); Dec: December; Jan: January; Mar: March; Apr: April

Figure 2. Leaf and fruit samples of: A. *Prunus mume* accession; and B. *Prunus salicina* accession. From left to right, showing fruit color changes from green to full ripening (n = 10)

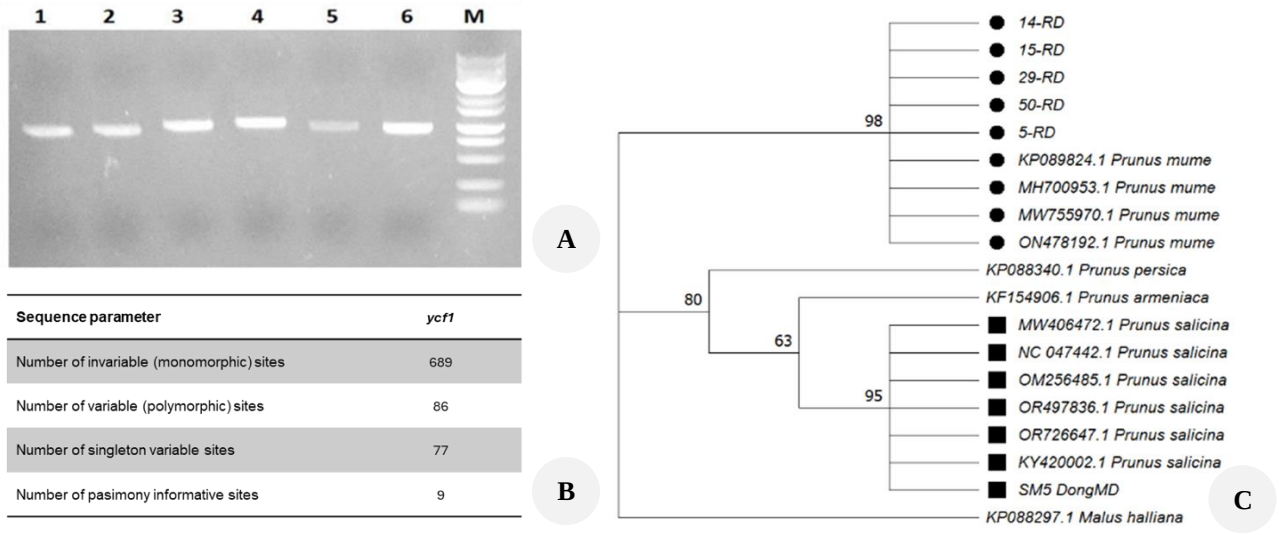

Sequence parameter	*ycf1*
Number of invariable (monomorphic) sites	689
Number of variable (polymorphic) sites	86
Number of singleton variable sites	77
Number of pasimony informative sites	9

Figure 3. A. Visualization of PCR amplified products of the *ycf1* gene of 6 *Prunus* spp. samples. (1-5) *P. mume* samples; (6) *P. salicina* sample. M: Ladder 1kb; B. Nucleotide sequence parameters for *ycf1* region based on the calculation of Mega X software; C. Phylogenetic tree by Maximum Likelihood of similarity between *Prunus mume* and other *Prunus* spp. based on *ycf1* sequences (Ln Likelihood = -1780.60)

DNA barcoding

Before assessing the genetic diversity and population structure of Japanese apricot germplasm (30 collected accessions), it was necessary to first identify and distinguish *P. mume* from other *Prunus* species. This study initially applied to six accessions (five *P. mume* accessions and one *P. salicina* accession). These accessions were analyzed using hypervariable regions of the chloroplast genome, specifically the *ycf1*, as candidate DNA barcodes. The result of amplification of the *ycf1* gene is presented in Figure 3.A. The result showed that the *ycf1* marker was successfully amplified in all six accessions (6/6), producing fragments of expected molecular weights (~970bp) and yielding high-quality sequencing results.

The *ycf1* gene lengths and nucleotide sequences of the six studied accessions, along with other *Prunus* species and the outgroup *Malus halliana* (sequencing data accessed from NCBI), were aligned and analyzed using MEGA X. A Maximum parsimony analysis of this alignment indicated 86 variable characters, including 9 parsimony-informative sites and 77 singleton sites (Figure 3.B). The phylogenetic tree obtained from Maximum likelihood (Lnlikelihood -1780.60) exhibited a distinct clade for *P. mume*, which consisted of the 5 analyzed accessions (5-RD, 14-RD, 15-RD, 29-RD, and 50-RD). This clade showed a sister relationship with the clade of *P. salicina*, which included the analyzed *P. salicina* accession (SM5 DongMD) with high bootstrap support (Figure 3.C).

The *ycf1* sequence data provided strong support for the monophyly of *P. mume* as a clade (98% bootstrap support: ML tree) and for *P. salicina* (95% bootstrap support in ML analysis) (Figure 3.C). Bootstrap values are given in appropriate clades. *P. mume* accessions include 5-RD, 14-RD, 15-RD, 29-RD, and 50-RD, while SM5 DongMD represents a *P. salicina* accession. Other *Prunus* accessions were sourced from the NCBI database for their *ycf1* sequences (*P. mume*: KP089824.1; MH700953.1; MW755970.1; ON478192.1; *P. salicina*: MW406472.1, NC047442.1; OM256485.1; OR497836.1; OR726647.1, KY420002.1). *Malus halliana* (KP088297.1) serves as an outgroup. *Prunus* is shown to be polyphyletic, with some species scattered throughout the topology. The monotypic species *P. armeniaca* and *P. persica* were separated from the *P. mume* accessions, receiving 63% and 80% bootstrap support, respectively (Figure 2.B). Pairwise divergences between the five studied *P. mume* accessions and other *P. mume* accessions were 0.000, while divergences with other species varied from 0.003 to 0.117% (Supplementary Data, Table S2). *Prunus mume* accessions were clearly distinguished from *P. salicina* accessions by 9 autapomorphic characters (Supplementary Data, Table S3), found only in one species but not the other. These autapomorphic characters refer to specific nucleotides (C, G, T, and A) in the *ycf1* gene sequence found only in *P. mume* but not in *P. salicina* based on sequence alignment. This result is consistent with the findings of Coulibaly et al. (2022) and Huang et al. (2022a), who indicated that the *ycf1* sequence had high nucleotide diversity, making it a valuable marker for taxonomy analysis.

Genetic diversity among *P. mume* accessions

The 19 SSR maker loci used in this study are distributed across 8 linkage groups in the reference map. These SSR markers demonstrated high polymorphism rates in evaluating Japanese apricot genetic diversity (Numaguchi et al. 2019). Based on PCR results, 49 alleles were detected from the 19 SSR markers for 30 *P. mume* accessions. The results showed that all 19 markers exhibited a polymorphism rate of 100%, with the average number of alleles per locus being 2.58 (Table 4; Figure 4).

The high PIC index further shows the markers' ability to differentiate among accessions within the population effectively. The average PIC index for the SSR markers in this study was 0.41, which was lower than the PIC value reported by Numaguchi et al. (2019) in their genetic diversity study of the Japanese apricot population. In other studies, this index was higher as reported by Sheikh et al. (2021) (0.32) and almost similar to 0.44 reported by Savoia et al. (2023) in *P. armeniaca* accessions However, 9 out of 19 SSR markers indicated high information (PIC value >0.5), with 6 markers having a PIC value ≥0.60, namely PKMS75, PKMS149, PKMS193, PKMS187, PKMS191, and PKMS193 (Table 4). Another 7 SSR markers showed moderate information (PIC value = 0.25-0.50) (Botstein et al. 1980). These results confirmed that SSR markers were applied for the genetic analysis of the Japanese apricot in northern Vietnam. Subsequently, these polymorphic SSR markers were used to analyze variations among the Japanese apricot accessions in the two surveyed populations (from two ecological regions, Red River delta region-RD and Northern Mountain-NM).

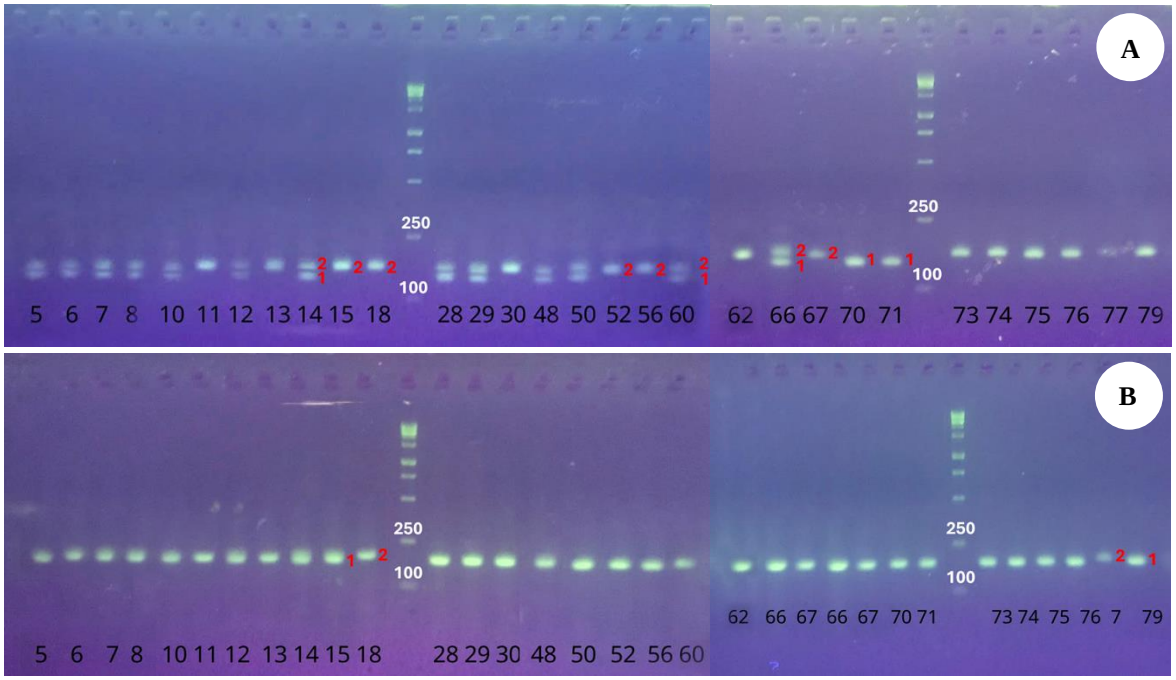

Figure 4. The banding pattern was generated by: A. PMKS175 primer; and B. PMKS121 primer. The individuals with the 1 or 2 scores predicted their genotypes. The numbers at the base of each well indicate the accession numbers corresponding to the accessions mentioned in Table 1. Numbers 5-50: Accessions collected from the RD region. Numbers 52-79: Accessions collected from the NM region

Table 4. Genetic diversity characteristics of 19 microsatellite loci used to assess 30 *Prunus mume* accessions collected from two ecological regions of northern Vietnam

Population	**Red River Delta (RD)**					**Northern Mountain Region (NM)**					**PIC**
SSR marker	N	N*a*	H*o*	H*e*	F*is*	N	N*a*	H*o*	H*e*	F*is*	
PMKS15	16	3	0.5	0.5	-0.09	14	1	0	0	~	0.34
PMKS 21	16	1	0	0	~	14	3	0.07	0.5	0.86	0.13
PMKS 49	16	2	0	0.22	1	14	3	0	0.54	1	0.24
PMKS 59	16	1	0	0	~	14	3	0	0.26	1	0.07
PMKS 68	16	3	0.06	0.44	0.86	14	3	0.07	0.2	0.64	0.45
PMKS 75	16	3	0.13	0.56	0.77	14	3	0	0.54	1	0.62
PMKS 99	16	1	0	0	~	14	2	0	0.41	1	0.54
PMKS 113	16	1	0	0	~	14	3	0.14	0.54	0.74	0.31
PMKS 121	16	2	0	0.12	1	14	2	0	0.25	1	0.24
PMKS 131	16	2	0.56	0.48	-0.17	14	2	0	0.14	1	0.51
PMKS 149	16	3	0.75	0.56	-0.35	14	3	0	0.57	1	0.6
PMKS 175	16	2	0.69	0.45	-0.52	14	2	0.14	0.34	0.58	0.47
PMKS 187	16	3	0.56	0.49	-0.16	14	3	0.5	0.48	-0.03	0.66
PMKS 197	16	2	0.06	0.06	-0.03	14	2	0.07	0.29	0.76	0.17
PMKS 193	16	3	0.56	0.53	-0.06	14	3	0.07	0.55	0.87	0.65
PMKS 164	16	3	0	0.4	1	14	2	0.07	0.48	0.85	0.51
PMKS 179	16	2	0.06	0.45	0.86	14	2	0	0.41	1	0.34
PMKS 133	16	2	0.69	0.45	-0.52	14	2	0.14	0.34	0.58	0.47
PMKS 191	16	3	0.38	0.56	0.32	14	3	0.07	0.4	0.82	0.76
Mean	16	2.21	0.26	0.33	0.26	14	2.47	0.07	0.38	0.81	0.41

Note: N*a*: No. of different alleles; H_O: Observed heterozygosity; H*e*: Expected heterozygosity; F*is*: Inbreeding coefficient; PIC: Polymorphism Information Content; ~: Allele monomorphic

Based on the SSR profile of the two collected populations, the average H_e value of the NM population (0.38) was higher than that of the RD population (0.33) (Table 4). These expected heterozygosity of *P. mume* were less than those reported for *P. mume* in Numaguchi et al. (2019) (0.81) and Wang et al. (2025) (0.769) and other *Prunus* species, such as *P. armeniaca* (0.585) and *P. persica* (0.626) (Savoia et al. 2023). This result indicated that the *P. mume* populations collected in northern Vietnam had a lower level of genetic diversity than populations in other regions. This provided the basis for the conservation and development of improved varieties for northern Vietnam. Meanwhile, the F*is* values of the RD and NM populations were in the range of -0.52 to 1.00 and -0.03 to 1, respectively. The average F*is* value for the NM (0.81) was higher than that of the RD population (0.26). Both the average F*is* values were higher than the F*is* value reported for the apricot population in the study by Numaguchi et al. (2019), indicating a deficiency in heterozygosity among the remaining apricot accessions. This confirmed that the impact of artificial selection has reduced genetic diversity in the *P. mume* population, as shown in the study of Huang et al. (2022b), that the genetic diversity index of the bred population is lower than that of the wild or domesticated Japanese apricot population. Therefore, this highlights the urgent need for conservation efforts for these apricot accessions.

Genetic differentiation among *P. mume* accessions was analyzed using Principal Coordinate Analysis (PCoA) based on genetic distances. The percentages of variation explained by PC1 and PC2 were 24.37% and 14.88%, respectively. PCoA identified two distinct groups based on their ecological location: RD (lower coordinate) and NM (upper coordinate) (Figure 5). The RD accessions, represented by green squares, were grouped into RD (population 1), while the NM accessions, represented by red rhombus shapes, were grouped into NM (population 2). For PC1 (24,37%), the accessions 6-RD,7-RD, 8-RD, 10-RD, 14-RD, 18-RD, 28-RD, 29-RD, and 48-RD located at Red River Delta showed clear genetic differentiation from the remaining accessions. However, five RD accessions (11-RD, 13-RD, 15-RD, 30-RD, and 50-RD) were separated from other RD accessions and appeared at the lower left coordinate. These five RD accessions showed slight differences compared to four NM accessions (52-NM, 56-NM, 62-NM, and 74-NM), which were positioned separately from the others in Population RD and NM. The exchange of genetic resources could explain this, as some growers have brought accessions from different geographic regions for cultivation. For example, accessions 11-RD, 13-RD, 15-RD, and 30-RD originated from the NM region and were grown in the RD region. This result is somewhat similar to the results of Hayashi et al. (2008), which showed genetic differences between Japanese apricot accessions from the northern region of China and Japan compared to those from southern subtropical areas like Thailand and Taiwan. Similar findings were also reported in the apricot study conducted by Bourguiba et al. (2020) using PCoA analysis. Bourguiba et al. (2020) grouped the accessions into five populations with different geographic regions of origin in the PCoA chart. The second axis distinguishes accessions from the East Asian and Central Asian groups from the rest of the populations. In addition, the observed cluster distribution also reflects accessions with the overlap between population 3 and population 5.

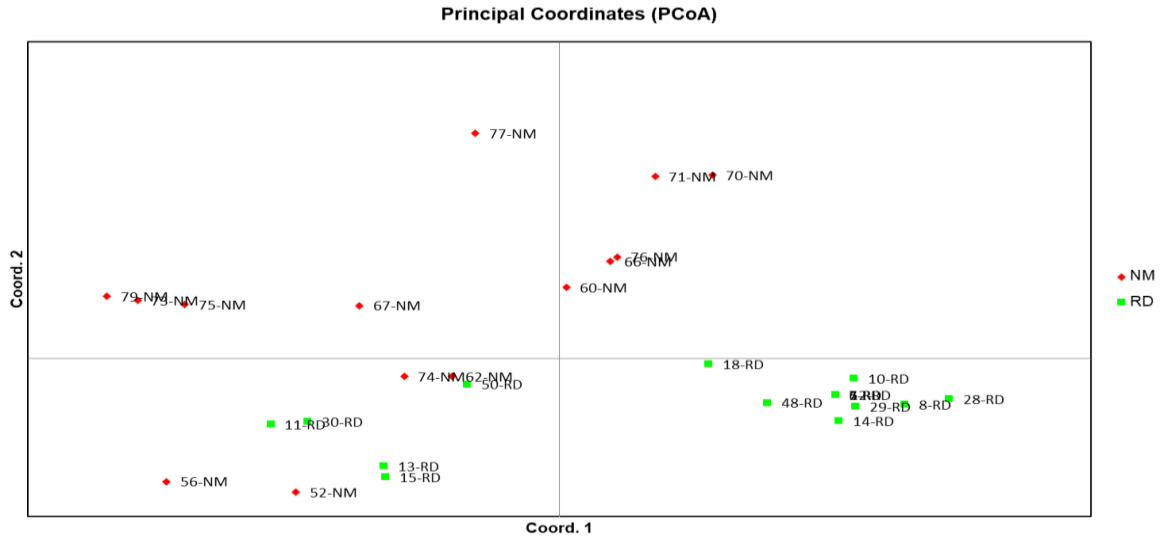

Figure 5. Principal coordinate analysis (PCoA) based on genetic distances among 30 *P. mume* accessions from 19 microsatellite markers (Green: Population 1 (RD); Red: Population 2 (NM); Accession number referred to Table 1)

Genetic structure of *P. mume* accessions

Population structure was analyzed based on 19 microsatellites, and the 30 *P. mume* accessions were grouped into 2 clusters (red and green colors in Figure 6.A). The number of clusters was determined by the K value, which indicates the number of clusters with the highest probability. To determine the best K, we used an ad hoc quantity (ΔK). The peak in the ΔK values (highest ΔK value = 89.251905) indicated the most likely number of optimal groups at K = 2 (Figure 6.B). So that the highest probability was observed at K = 2, indicating that the 30 *P. mume* accessions can be classified into two clusters (Figure 6.A). Each vertical line represents an accession, with a different color indicating the estimated membership coefficient (Q) to the respective group. The red and green colors represent the members of 2 populations inferred by the STRUCTURE harvester (Group 1 (Pop 1)-red color with 12 accessions; Group 2 (Pop 2- green color with 18 accessions). These two populations comprised accessions collected from two geographic regions, suggesting cultivar introduction or movement among areas.

The first cluster (labeled red, denoted as Pop 1) contained 12 accessions, mostly from the northern mountain regions of Vietnam (Figure 6.A). As seen in the PCoA results, four accessions (11-RD, 13-RD, 15-RD, and 30-RD), collected from the Red River delta, were assigned to Pop 1 but originated from the mountainous areas. The second cluster (labeled green, denoted as Pop 2) consisted of 18 accessions (5-RD, 6-RD, 7-RD, 8-RD, 10-RD, 12-RD, 14-RD, 18-RD, 28-RD, 29-RD, 48-RD, 50-RD, 60-NE, 66-NW, 67-NW, 71-NW, 74-NW, 75-NW), most of which were collected from Hanoi province in the Red River Delta region (RD). The number of populations detected in this study is consistent with the findings of Numaguchi et al. (2019), who used microsatellite markers and STRUCTURE analysis to separate 94 *P. mume* accessions into two groups. Similarly, Hayashi et al. (2008) used UPGMA analysis to group 127 *P. mume* germplasm into three major clusters, with two clusters derived from subtropical germplasm from Taiwan and Thailand. Previous results showed the relationship between geographic regions of origin and the genetic structure of germplasm on some fruits like apricot (*P. armeniaca*) and date palm (*Phoenix dactylifera*) (Zehdi-Azouzi et al. 2015; Bourguiba et al. 2020; Hudcovicová et al. 2025). Bourguiba et al. (2020) and Hudcovicová et al. (2025) also showed that the common apricot accessions were arranged according to their geographic origin. Bourguiba et al. (2020) showed that five populations were generated from 890 common apricot accessions from different geographic regions of origin, such as eastern Asia, Continental Europe, Central Asia and China, Mediterranean Europe, and North Africa, Irano-Caucasia and North Africa.

Additionally, each accession was represented by a vertical bar, with the length of the colored segments indicating the accession's estimated membership fraction (Q) in each population. Accessions were assigned to a specific population if the highest Q was higher than 0.9. Twenty-nine of the 30 accessions had Q>0.9, indicating they were genetically pure or had limited genetic exchanges with other accessions. However, accession 50-RD (serial number 16) exhibited genetic admixture, as noted in a Q value of <0.90, suggesting the potential influence of other accessions on their origin (Figure 6.A). This can appear when there is a cross between cultivars, as in the study of Zhebentyayeva et al. (2008), which showed that the resistance to plum pox virus in the North American gene pool also originated in China. Bourguiba et al. (2020) reported that the collected American accessions are genetic admixtures contributed by two other gene pools. Slovakian cultivar 'Barbora' was shown as a combination of 'Madarska' and Central Asian cultivars (Hudcovicová et al. 2025). Therefore, 50-RD accession can also be a hybrid between the apricot cultivar of the Red River Delta (RD) and the Northern Mountain (NM).

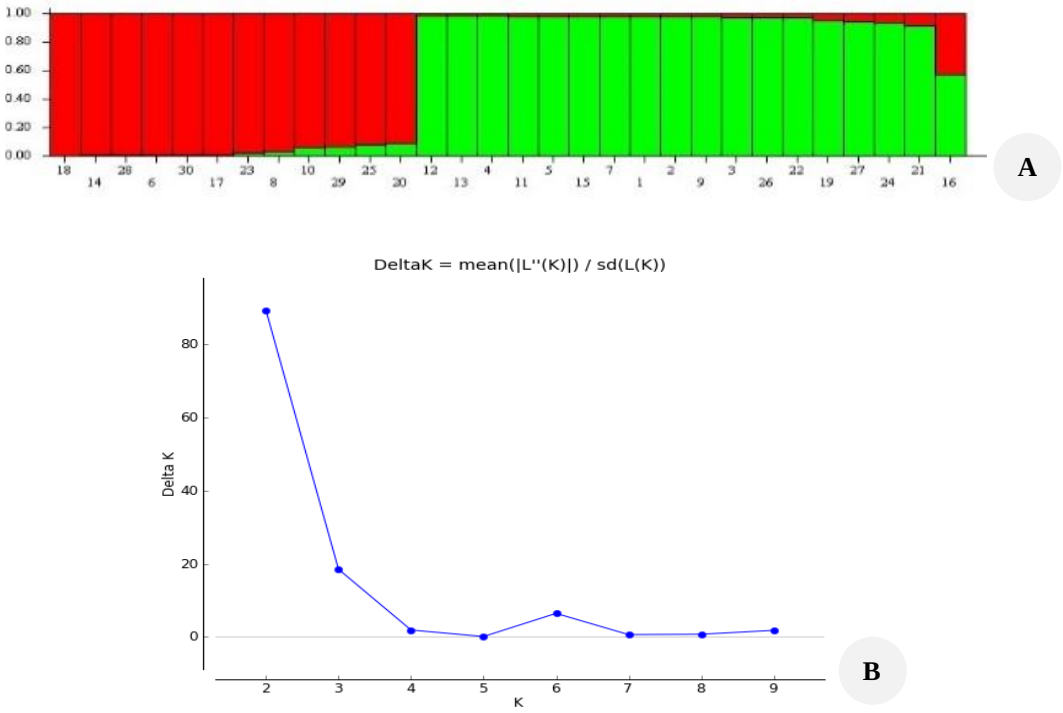

Figure 6. Structure harvester and Delta K value elucidated using Evanno et al. (2005) method and Bayesian model-based valuation of population structure of 30 *P. mume* accessions based on 19 microsatellite markers: A. Bar plot represented for K = 2: 30 accessions are divided into 2 subpopulations; B. Determinations of subpopulations K based on maximum ΔK values: K = 2 indicates the maximum ΔK value (highest ΔK value = 89.251905). The numbers at the base of each vertical line indicate the serial numbers corresponding to the accessions mentioned in Table 1

In conclusion, the *P. mume* accessions were identified and distinguished from *P. salicina* accessions based on a sequence of the *ycf1* gene located in the chloroplast genome and several agro-morphological traits. In comparison with *P. salicina* accessions, *P. mume* exhibited a later flowering time (in January), shorter leaf length, smaller fruit size, and a lower flesh rate but higher total soluble solid content in the fruits. The 19 SSR primers generated polymorphic markers across 30 Japanese apricot accessions in northern Vietnam. Nine out of 19 SSR markers indicated high information, with a PIC value >0.5. Based on SSR genotyping data, these accessions were clustered into two populations (RD and NM) according to Structure and PCoA analysis, reflecting their geographic region of origin. The average He value for the NM population was higher than that of the RD population, indicating the higher genetic diversity in the NM population. 50-RD may be a hybrid accession between the cultivars from the RD population and the NM population. The findings from this study provide valuable insights and methods for identifying *P. mume* species and evaluating genetic variation, which will aid in managing *P. mume* germplasm resources and breeding programs in Vietnam.

ACKNOWLEDGEMENTS

We are grateful to Assoc. Prof. Dr. Ha Viet Cuong (Vietnam National University of Agriculture) for technical assistance and his useful discussion, Mr. Vuong Ngoc Kien and Mr. Le Manh Dong (My Duc district, Hanoi Province) for kindly providing samples. We also thank the Fundamental Research Funds of Vietnam National University of Agriculture, Vietnam, for funding Project No. T2021-01-03TD to complete this manuscript.

REFERENCES

Amar MH. 2020. ycf1-ndhF genes, the most promising plastid genomic barcode, sheds light on phylogeny at low taxonomic levels in *Prunus persica*. J Genet Eng Biotechnol 18 (1): 42. DOI: 10.1186/s43141-020-00057-3.

Bourguiba H, Scotti I, Sauvage C, Zhebentyayeva T, Ledbetter C, Krška B, Remay A, D'Onofrio C, Iketani H, Christen D, Krichen L, Trifi-Farah N, Liu W, Roch G, Audergon J-M. 2020. Genetic structure of a worldwide germplasm collection of *Prunus armeniaca* L. reveals three major diffusion routes for varieties coming from the species' center of origin. Front Plant Sci 11: 638. DOI: 10.3389/fpls.2020.00638.

Batnini MA, Bourguiba H, Trifi-Farah N, Krichen L. 2019. Molecular diversity and phylogeny of Tunisian *Prunus armeniaca* L. by evaluating three candidate barcodes of the chloroplast genome. Sci Hortic 245: 99-106. DOI: 10.1016/j.scienta.2018.09.071.

Botstein D, White RL, Skolnick M, Davis RW. 1980. Construction of a genetic linkage map in man using restriction fragment length polymorphisms. Am J Hum Genet 32 (3): 314-331.

Chen J, Liu Q, Lu C, Liu Q, Pan J, Zhang J, Dong S. 2022. Genetic diversity of *Prunus armeniaca* L. var. ansu Maxim. germplasm revealed by Simple Sequence Repeat (SSR) markers. PLoS One 17 (6): e0269424. DOI: 10.1371/journal.pone.0269424.

Coulibaly D, Huang X, Ting S, Iqbal S, Ni Z, Ouma KO, Hayat F, Tan W, Hu G, Ma C, Karikari B, Magdy M, Gao Z. 2022. Comparative analysis of complete chloroplast genome and phenotypic characteristics of

Japanese apricot accessions. Horticulturae 8 (9): 794. DOI: 10.3390/horticulturae8090794.
Dettori MT, Micali S, Giovinazzi J, Scalabrin S, Verde I, Cipriani G. 2015. Mining microsatellites in the peach genome: Development of new long-core SSR markers for genetic analyses in five *Prunus* species. SpringerPlus 4: 337. DOI: 10.1186/s40064-015-1098-0.
Dong W, Xu C, Li C, Sun J, Zuo Y, Shi S, Cheng T, Guo J, Zhou S. 2015. *ycf1*, the most promising plastid DNA barcode of land plants. Sci Rep 5: 8348. DOI: 10.1038/srep08348.
Evanno G, Regnaut S, Goudet J. 2005. Detecting the number of clusters of individuals using the software STRUCTURE: A simulation study. Mol Ecol 14 (8): 2611-2620. DOI: 10.1111/j.1365-294x.2005.02553.x.
Gao Z-H, Shen Z-J, Han Z-H, Fang J-G, Zhang Y-M, Zhang Z. 2004. Microsatellite markers and genetic diversity in Japanese apricot (*Prunus mume*). HortScience 39 (7): 1571-1574. DOI: 10.21273/hortsci.39.7.1571.
Gao X, Wu S, Lv G, Wang M, Li L, Liu Y, He F, Xiao J. 2025. The key metabolic genes and networks regulating the fruit acidity and flavonoid of *Prunus mume* revealed via transcriptomic and metabolomic analyses. Front Plant Sci 16: 1544500. DOI: 10.3389/fpls.2025.1544500.
Guerrero BI, Guerra ME, Rodrigo J. 2022. Simple Sequence Repeat (SSR)-based genetic diversity in interspecific plumcot-type (*Prunus salicina* × *Prunus armeniaca*) hybrids. Plants 11 (9): 1241. DOI: 10.3390/plants11091241.
Halász J, Szendy G, Ivanovska B, Tóth EG, Hegedűs A. 2023. The self-incompatibility locus and chloroplast DNA regions of *Prunus domestica* reflect the origin and genetic diversity of traditional cultivars. J Amer Soc Hort Sci 148 (5): 230-239. DOI: 10.21273/jashs05330-23.
Hayashi K, Shimazu K, Yaegaki H, Yamaguchi M, Iketani H, Yamamoto T. 2008. Genetic diversity in fruiting and flower-ornamental Japanese apricot (*Prunus mume*) germplasms assessed by SSR markers. Breed Sci 58 (4): 401-410. DOI: 10.1270/jsbbs.58.401.
Hürkan K. 2020. Analysis of various DNA barcodes on the Turkish protected designation of origin apricot "Iğdır Kayısısı" (*Prunus armeniaca* cv. Şalak). Turkish J Agric Food Sci Technol 8 (9): 1982-1987. DOI: 10.24925/turjaf.v8i9.1982-1987.3594.
Huang X, Coulibaly D, Tan W, Ni Z, Shi T, Li H, Hayat F, Gao Z. 2022a. The analysis of genetic structure and characteristics of the chloroplast genome in different Japanese apricot germplasm populations. BMC Plant Biol 22 (1): 354. DOI: 10.1186/s12870-022-03731-5.
Huang X, Ni Z, Shi T, Tao R, Yang Q, Luo C, Li Y, Li H, Gao H, Zhou X, Xu L, Gao Z. 2022b. Novel insights into the dissemination route of Japanese apricot (*Prunus mume* Sieb. et Zucc.) based on genomics. Plant J 110 (4): 1182-1197. DOI: 10.1111/tpj.15731.
Hudcovicová M, Klčová L, Gubišová M, Gubiš J, Zetochová E, Horacek M, Kraic J, Havrlentová M, Ondreičková K. 2025. Genetic diversity in apricot orchards across key growing regions in Slovakia and Austria, along with cultivar authentication of apricot genotypes found in the market. Appl Sci 15 (5): 2444. DOI: 10.3390/app15052444.
Kumar R, Dimri DC, Karki K, Rai KM, Singh NK, Shivran JS, Bharti S. 2023. SSR marker based profiling and population structure analysis in peach (*Prunus persica*) germplasm. Indian J Agric Sci 93 (10): 1080-1085. DOI: 10.56093/ijas.v93i10.132658.
Li M, Zheng P, Ni, B, Hu X, Miao X, Zhao Z. 2018. Genetic diversity analysis of apricot cultivars grown in China based on SSR markers. Eur J Hortic Sci 83 (1): 18-27. DOI: 10.17660/ejhs.2018/83.1.3.
Li M, Sang M, Wen Z, Meng J, Cheng T, Zhang Q, Sun L. 2022. Mapping floral genetic architecture in *Prunus mume*, an ornamental woody plant. Front Plant Sci 13: 828579. DOI: 10.3389/fpls.2022.828579.
Liu Z, Yang Y, Sun C, Wu Y, Li X. 2022. Comparative phytochemical property and antioxidant activity of sixteen Mei (*Prunus mume*) fruit cultivars from six provinces in China. Intl J Food Prop 25 (1): 617-633. DOI: 10.1080/10942912.2022.2053707.
Moore R, Yoneda K. 2022. 1029. *Prunus mume*: Rosaceae. Curtis's Bot Mag 39 (3): 409-431. DOI: 10.1111/curt.12455.
Morimoto T, Kitamura Y, Numaguchi K, Akagi T, Tao R. 2019. Characterization of post-mating interspecific cross-compatibility in *Prunus* (Rosaceae). Sci Hortic 246: 693-699. DOI: 10.1016/j.scienta.2018.11.045.
Morimoto T, Murai Y, Yamauchi R, Kitamura Y, Numaguchi K, Itai A. 2022. Phenotypic diversity of organic acids, sugars and volatile compounds associated with subpopulations in Japanese apricot (*Prunus mume*) cultivars. Hortic J 91: 1-9. DOI: 10.2503/hortj.UTD-301.
Moustafa K, Cross J. 2019. Production, pomological and nutraceutical properties of apricot. J Food Sci Technol 56 (1): 12-23. DOI: 10.1007/s13197-018-3481-7.
Nguyen HH. 2024. Diversity of Japanese apricot genetic resources in Vietnam. Proceedings of the Workshop on the History of cultivation, development and cultural values of Huong Tich apricot. Vietnam National University of Agriculture, Hanoi, 25 January 2024. [Vietnamese]
Numaguchi K, Ishio S, Kitamura Y, Nakamura K, Ishikawa R, Ishii T. 2019. Microsatellite marker development and population structure analysis in Japanese apricot (*Prunus mume* Sieb. et Zucc.). Hortic J 88 (2): 222-231. DOI: 10.2503/hortj.utd-013.
Numaguchi K, Akagi T, Kitamura Y, Ishikawa R, Ishii T. 2020. Interspecific introgression and natural selection in the evolution of Japanese apricot (*Prunus mume*). Plant J 104 (6): 1551-1567. DOI: 10.1111/tpj.15020.
Numaguchi K, Kitamura Y, Kashiwamoto T, Morimoto T, Oe T. 2023. Genomic region and origin for selected traits during differentiation of small-fruit cultivars in Japanese apricot (*Prunus mume*). Mol Genet Genomics 298 (6): 1365-1375. DOI: 10.1007/s00438-023-02062-w.
Peakall R, Smouse PE. 2012 GenAlEx 6.5: Genetic analysis in Excel. Population genetic software for teaching and research-An update. Bioinformatics 28 (19): 2537-2539. DOI: 10.1093/bioinformatics/bts460.
POWO [Plants of the World Online]. 2025. The World Checklist of Vascular Plants. https://powo.science.kew.org/. [21 March 2025]
Pritchard JK, Stephens M, Donnelly P. 2000. Inference of population structure using multilocus genotype data. Genetics 155 (2): 945-959. DOI: 10.1093/genetics/155.2.945.
Savoia MA, Del Faro L, Turco A, Fanelli V, Venerito P, Montemurro C, Sabetta W. 2023. Biodiversity evaluation and preservation of Italian stone fruit germplasm (peach and apricot) in southern Italy. Plants 12 (6): 1279. DOI: 10.3390/plants12061279.
Sayed HA, Mostafa S, Haggag IM, Hassan NA. 2023. DNA barcoding of *Prunus* species collection conserved in the National Gene Bank of Egypt. Mol Biotechnol 65 (3): 410-418. DOI: 10.1007/s12033-022-00530-z.
Sevindik E, Korkom Y, Murathan ZT. 2024. Evaluating DNA barcoding using cpDNA *matK* and *rbcL* for species identification and phylogenetic analysis of *Prunus armeniaca* L. (Rosaceae) genotypes. Genet Resour Crop Evol 71: 1825-1835. DOI: 10.1007/s10722-023-01748-9.
Sheikh ZN, Sharma V, Shah RA, Raina S, Aljabri M, Mir JI, AlKenani N, Hakeem KR. 2021. Elucidating genetic diversity in apricot (*Prunus armeniaca* L.) cultivated in the north-western Himalayan Provinces of India using SSR Markers. Plants 10 (12): 2668. DOI: 10.3390/plants10122668.
Student. 1908. The probable error of a mean. Biometrika 6 (1): 1-25. DOI: 10.1093/biomet/6.1.1.
Suwannachot J, Ketnawa S, Ogawa Y. 2021. Comparative study of the physico- and biochemical properties of two types of salted Japanese apricot (*Prunus mume*) pickles. Front Sustain Food Syst 5*:* 606688. DOI: 10.3389/fsufs.2021.606688.
Wang Z, Zhou D, Zhao Y, Tong Y, Zheng W, Li Q. 2025. Genetic diversity and molecular identity of *Prunus mume* with both ornamental and edible values based on fluorescence-labeled Simple Sequence Repeat (SSR) markers**.** Sheng Wu Gong Cheng Xue Bao 41 (2): 639-656. DOI: 10.13345/j.cjb.240676. [Chinese]
Xue S, Shi T, Luo W, Ni X, Iqbal S, Ni Z, Huang X, Yao D, Shen Z, Gao Z. 2019. Comparative analysis of the complete chloroplast genome among *Prunus mume*, *P. armeniaca*, and *P. salicina*. Hortic Res 6: 89. DOI: 10.1038/s41438-019-0171-1.
Yaegaki H, Haji T, Nakamura Y, Miyake M, Nishimura K, Kyotani H, Yamaguchi M. 2003. Variety and yearly variations of fruit and endocarp weights and their ratio in Japanese apricot (*Prunus mume* Sieb. et Zucc.) cultivars. J Japan Soc Hort Sci 72 (6): 546-550. DOI: 10.2503/jjshs.72.546.
Yoon SH, Koh E, Choi B, Moon B. 2019. Effects of soaking and fermentation time on biogenic amines content of maesil (*Prunus mume*) extract. Foods 8 (11): 592. DOI: 10.3390/foods8110592.
Zehdi-Azouzi S, Cherif E, Moussouni S et al. 2015. Genetic structure of the date palm (*Phoenix dactylifera*) in the Old World reveals a strong differentiation between eastern and western populations. Ann Bot 116 (5): 847. DOI: 10.1093/aob/mcv132.
Zhebentyayeva TN, Reighard GL, Lalli D, Gorina VM, Krška B, Abbott AG. 2008. Origin of resistance to *plum pox virus* in Apricot: What new AFLP and targeted SSR data analyses tell. Tree Genet Genomes 4: 403-417. DOI: 10.1007/s11295-007-0119-8.